Dynamics of thin jets generated by temperature fronts

V. P. Goncharov

A. M. Obukhov Institute of Atmospheric Physics RAS, 109017 Moscow, Russia

The path equations are derived to describe the nonlinear evolution of thin jets generated by temperature fronts. An approximate approach is based on the thermal rotating shallow-water model that accounts for the effect of the temperature gradient and uses the variational principle of least action. The dynamics of jets is shown to be effectively described by a nonlinear system of two $(1 + 1)$-dimensional partial differential equations. Particular solutions are found in the form of a steady-state meandering jet, a cusped jet, and a two-armed spiral.

I. INTRODUCTION

As is known, horizontal pressure gradients, typically occurring at frontal interfaces in the atmosphere and ocean, cause jet currents. The dynamics of such jets have attracted and continue to attract much attention in the scientific literature [1–9] for more than fifty years. Despite using various approaches and accounting for beta and topographic effects, the analytical study of the dynamics of frontal jets so far has been limited to the study of jets arising only at the fronts of potential vorticity (PV). Theoretical approaches to the study of the trajectory dynamics of jets generated at temperature fronts are lacking.

In the most advanced (sophisticated) models devoted to the PV-frontal jets, their description can be simplified to such an extent under certain assumptions that it reduces to formulating the so-called "path equations." The path-dynamic equations follow from these models in the thin-jet approximation when the typical radius of curvature of the jet midline becomes large compared with the Rossby radius of deformation. In essence, results obtained by Refs. [6–8] shown that, under rather general conditions, the evolution of a jet path obeys the modified Korteweg-de Vries equation formulated in terms of path curvature as a function of time and arc length.

It would be extremely curious and logical to implement a similar lumped approach to describe jets arising not on gradients of potential vorticity but on temperature gradients. That is what the given work aims for and, to reach it, we will use the thermal rotating shallow water (TRSW) [10–12] model. In geophysical fluid dynamics, this model is used to describe depth-averaged columnar motions of a horizontally nonhomogeneous fluid in a shallow active layer. The TRSW model, as inherently conservative, is capable of reproducing frontal effects for both potential vortex and temperature (buoyancy), and it is convenient because it makes them easy to control.

The paper is organized as follows: In Sec. II, we present a general description of the TRSW model for an active atmospheric layer and formulate a variational (Hamilton's) principle of least action for it. In Sec. III, within the framework of the Lagrangian approach, we derive the path equations which describe the dynamics of thin jets along the zero-buoyancy lines marking temperature fronts. Some particular solutions of these nonlinear path equations are considered in Sec. IV. In Sec. V, we discuss results obtained. The Appendix addresses the stability of some solutions.

---

*v.goncharov@rambler.ru

103801-1

II. THERMAL ROTATING SHALLOW WATER MODEL FOR ACTIVE ATMOSPHERIC LAYER

The TRSW model for the active atmospheric layer is formulated in the hydrostatic approximation and neglects dissipation. All kinetic energy is assumed to be determined mainly by horizontal motions and concentrated in a sufficiently narrow horizontally temperature-inhomogeneous boundary layer of height $h(x, y, t)$ above which there is a weakly perturbed, almost homogeneous fluid. This model, whose complete derivation in the context of the boundary layer in the atmosphere can be found in Refs. [10–13] and is governed by the equations

$$\frac{Du}{Dt} - fv = -bh_x - \frac{1}{2}hb_x, \tag{1}$$

$$\frac{Dv}{Dt} + fu = -bh_y - \frac{1}{2}hb_y, \tag{2}$$

$$\frac{Dh}{Dt} + h(u_x + v_y) = 0, \tag{3}$$

$$\frac{Db}{Dt} = 0. \tag{4}$$

The notations are as follows: x, y are the horizontal Cartesian coordinates, t is the time, subscripts denote the partial derivatives, u, v are the depth-averaged components of the horizontal velocity, $f(x, y)$ is the Coriolis parameter, and $D/Dt = \partial_t + u\partial_x + v\partial_y$ is the total derivative.

Equations (1)–(4) describe the depth-averaged flow of horizontally nonuniform fluid which is in a boundary layer of thickness $h(x, y, t)$ under the influence of gravity and the Coriolis force. So the terms fv and fu on the left side of Eqs. (1) and (2) imply the components of the Coriolis acceleration.

In deriving Eqs. (1)–(4), we assume that the lower layer is horizontally nonhomogeneous with density $\varrho_0 + \Delta\varrho$, while the upper layer is spanned to infinity and filled with an incompressible homogeneous fluid with density ϱ_0. In this case, the variable b has a meaning of relative buoyancy and is defined as

$$b = g\Delta\varrho/\varrho_0, \tag{5}$$

where g is gravity, and $\Delta\varrho(x, y, t)$ is the density deviation from the background value ϱ_0.

When density variations are induced only by temperature variations θ and to each other are linearly connected, the relative buoyancy can be computed as

$$b = -g\Delta\theta/\theta_0, \tag{6}$$

where $\Delta\theta(x, y, t)$ is the variable part and θ_0 is a reference value for the potential temperature. This parametrization allows taking into account both heating and cooling effects (see, for example, Refs. [14,15]).

The model (1)–(4) conserves the integral of total energy:

$$\mathcal{H} = \frac{1}{2} \int h(u^2 + v^2 + hb)dxdy, \tag{7}$$

and, like any other nondissipative mechanical systems, admits a variational (Hamilton's) principle of least action, which, following Refs. [16,17], can be formulated as

$$\delta S = 0, \quad S = \int \mathcal{L}dt, \tag{8}$$

where S is the action and $\mathcal{L}$ is the Lagrangian given by

$$\mathcal{L} = \int h[u(u - R) + v(v + P)]dxdy - \mathcal{H}, \tag{9}$$

where $R(x, y)$ and $P(x, y)$ are any two functions satisfying the condition

$$R_y + P_x = f(x, y). \tag{10}$$

According to what variables are chosen as dependent and independent, and what restrictions are used, based on Eqs. (8) and (9), it is possible to obtain different versions of the variational principle. In this paper, we use a Lagrangian version by considering the position

$$x = \hat{x}(s, n, t), \quad y = \hat{x}(s, n, t), \tag{11}$$

of fluid particles as functions of curvilinear labeling coordinates (s, n) and time t.

Since the labeling coordinates remain constant for any fluid particle during its columnar motion, the transformation (11) provides the rules

$$\frac{DF}{Dt} = \hat{F}_t, \quad F_x = \frac{1}{J}[\hat{F}, \hat{x}], \quad F_y = -\frac{1}{J}[\hat{F}, \hat{y}]. \tag{12}$$

Here the hat symbol indicates that arguments of a function are taken at $x = \hat{x}, y = \hat{y}$:

$$\hat{F} = F|_{x=\hat{x}, y=\hat{y}}, \tag{13}$$

and square brackets $[.,.]$ denote the bilinear operator:

$$[A, B] = A_s B_n - A_n B_s, \tag{14}$$

which at $A = \hat{x}, B = \hat{y}$ yields the Jacobian for the transformation (11):

$$J = [\hat{x}, \hat{y}]. \tag{15}$$

Thus, in the labeling coordinates, with the account of (12), the velocities are transformed by the rules

$$\hat{u} = \frac{Dx}{Dt} = \hat{x}_t, \quad \hat{v} = \frac{Dy}{Dt} = \hat{y}_t, \tag{16}$$

and Eqs. (3) and (4) take the form

$$\partial_t(J\hat{h}) = 0, \quad \hat{b}_t = 0. \tag{17}$$

Because Eqs. (17) are true for any choice of the labeling coordinates, it is convenient to assign them so that equal areas in (s, n) space contain equal volumes:

$$H ds dn = h dx dy, \tag{18}$$

where the constant H is the average layer depth. Then the integration of Eqs. (17) over time leads us to the constraints

$$J\hat{h} = H, \quad \hat{b} = B(s, n). \tag{19}$$

Here the function B is defined by the initial buoyancy distribution and, hence, depends only on s and n.

Now, we can apply the transformation (11) directly to the Lagrangian (9). By using the relations (16), (18), and (19), we find

$$\mathcal{L} = \frac{H}{2} \int \left(\hat{x}_t^2 + \hat{y}_t^2 - 2\hat{R}\hat{x}_t + 2\hat{P}\hat{y}_t - H\frac{B}{J} \right) ds dn, \tag{20}$$

where

$$\hat{R} = R(\hat{x}, \hat{y}), \quad \hat{P} = P(\hat{x}, \hat{y}). \tag{21}$$

The variation of this Lagrangian with respect to $\hat{x}$ and $\hat{y}$ under constraint (10) leads us to the closed system of equations

$$\hat{x}_{tt} - \hat{f}\hat{y}_t = -\frac{H}{2}\Big[\frac{B}{J^2}, \hat{y}\Big], \tag{22}$$

$$\hat{y}_{tt} + \hat{f}\hat{x}_t = \frac{H}{2}\Big[\frac{B}{J^2}, \hat{x}\Big]. \tag{23}$$

III. PATH EQUATION FOR THIN JETS

The thin-jet approximation used to obtain the so-called path equations describing the midline dynamics of jets relies on a philosophy typical of constructing models with lumped parameters. A general approach to similar problems can be implemented within the framework of adiabatic perturbation theory. In our particular case, we proceed from the assumption that the transverse size of jets is small compared with the characteristic scale of horizontal changes.

In doing so, in the zeroth approximation, we clarify the structural elements of the theory, and, at the next stage, find out the character of their evolution or interaction. Variants of such an approach have been used previously in soliton theory [18], superconductivity [19], quantum field theory [20], and in the theory of dissipative vortices [21].

To not overload the analysis with unessential details, at least for the first order of perturbation theory, we consider a simplified model assuming that

$$f = \text{const}., \quad h = H = \text{const}. \tag{24}$$

Then, Eqs. (1)–(4) have a stationary solution

$$v = 0, \quad u = -\frac{H}{2f}b_y, \tag{25}$$

where the variables u and b are functions only of y.

Since b is the relative buoyancy, in the case of a jump-wise variation initiated by a temperature front, it changes sign, and Eq. (25) describes a jet flow localized along the x axis. In particular, the assumption that

$$b = b^* \tanh\left(\frac{y}{l}\right), \quad b^* = g\frac{\Delta\theta^*}{\theta_0}, \tag{26}$$

leads us to the Bickley jet with velocity profile

$$u = -u^* \text{sech}^2\left(\frac{y}{l}\right), \quad u^* = \frac{Hb^*}{2fl}. \tag{27}$$

Here l is the width of the jet, u^* is a peak value of the velocity at the jet axis, while b^* and $\Delta\theta^*$ are peak values attained, respectively, by buoyancy and by temperature deviation in a quiescent region far from the jet.

For conditions typical of Earth's atmosphere,

$$H \approx 4 \text{ km}, \quad g \approx 10 \text{ m s}^{-2}, \quad f \approx 10^{-4} \text{ s}^{-1}, \tag{28}$$

$$l \approx 20 \text{ km}, \quad \Delta\theta^*/\theta_0 \approx 5 \times 10^{-3}, \tag{29}$$

this formula gives an estimate $u^* \approx 50 \text{ m s}^{-1}$ that is quite consistent with the observations.

Similar solutions also exist in the Lagrangian version of the model if the buoyancy distribution B is a function only of n. As follows from Eqs. (22) and (23), such solutions look like

$$\hat{x} = s - u(n)t, \quad \hat{y} = n, \quad u(n) = \frac{H}{2f}B_n. \tag{30}$$

These examples show that the zero-buoyancy lines along which the jets move may well be suitable as structural elements of the theory.

To obtain the path equations describing the large-scale motions of zero-buoyancy lines, we further employ an approach based on the principle of least action. For this purpose, it is preferable to formulate the Lagrangian in a dimensionless form. As we see later, this way will allow us to estimate the order of the terms into the Lagrangian, to compare, and to neglect the smallest of them.

Since, in the case of constant Coriolis force, from (10) it follows that

$$R = \tfrac{1}{2}fy, \quad P = \tfrac{1}{2}fx, \tag{31}$$

using f^{-1} and the Rossby deformation radius

$$L = \left(\frac{gH\Delta\theta^*}{f^2\theta_0} \right)^{1/2} \tag{32}$$

as the natural scales of time and horizontal length, after transforming by the rules

$$(\hat{x}, \hat{y}, s, n) \rightarrow L(\hat{x}, \hat{y}, s, n), \tag{33}$$

$$t \rightarrow f^{-1}t, \quad B \rightarrow f^2L^2B, \quad \mathcal{L} \rightarrow f^2L^4\mathcal{L} \tag{34}$$

both dependent $\hat{x}$, $\hat{y}$, B and the independent s, n, t variables, so we find

$$\mathcal{L} = \frac{1}{2} \int \left(\hat{x}_t^2 + \hat{y}_t^2 - \hat{y}\hat{x}_t + \hat{x}\hat{y}_t - \frac{B}{J} \right) ds\,dn. \tag{35}$$

Let the jet be thin enough and localized at the zero-buoyancy line, which is described parametrically as

$$x = X(s, t), \quad y = Y(s, t). \tag{36}$$

The thin-jet approximation implies an expansion of the field variables in the vicinity of the jet trajectory, and it assumes that the dependent and independent variables appearing in the Lagrangian (35) have the following orders:

$$s \sim \hat{x} \sim \hat{y} \sim 1/\epsilon, \quad n \sim B \sim 1, \quad t \sim 1/\lambda, \tag{37}$$

where ϵ and $\lambda(\epsilon)$ are two small perturbation parameters. How they relate to each other will be found later. Note that, although the smallness of ϵ is arbitrary, it will be measured as the ratio $\epsilon \sim l/L$.

Then, expanding the functions $\hat{x}$ and $\hat{y}$ by powers of n and ϵ, one can find that

$$\hat{x} = \frac{1}{\epsilon}[X + \epsilon nX_1 + \epsilon^2 n^2 X_2 + O(\epsilon^3)], \tag{38}$$

$$\hat{y} = \frac{1}{\epsilon}[Y + \epsilon nY_1 + \epsilon^2 n^2 Y_2 + O(\epsilon^3)], \tag{39}$$

where $X_1(s, t)$, $Y_1(s, t)$ are the displacements in the first order of perturbation theory, and $X_2(s, t)$, $Y_2(s, t)$ are the displacements in the second order.

Similarly, we can find the expansion of buoyancy. Assuming that the velocity of the jet is localized in the vicinity of the zero buoyancy line and reaches its maximum at it, one can conclude that the function $B(s, n)$ must be odd with respect to n, so its expansion starts with a linear term

$$B = n\gamma + O(\epsilon^2). \tag{40}$$

Here the coefficient $\gamma(s)$ characterizing the across-jet temperature gradient (or the along-jet velocity) can depend only on the longitudinal coordinate s.

The Jacobian J is one more quantity that we should expand into a power series in ϵ. Substituting (33) into (14), it is easy to find

$$J = J_0 + n\epsilon J_1 + O(\epsilon^2), \tag{41}$$

$$J_0 = X_s Y_1 - Y_s X_1, \tag{42}$$

$$J_1 = X_{1s} Y_1 - Y_{1s} X_1 + 2(X_s Y_2 - Y_s X_2). \tag{43}$$

Now we can find a thin-jet approximation for the Lagrangian. To do this, lets use the expansions (38)–(41). By inserting them directly into the Lagrangian (35) and integrating it over $-1 \leqslant n \leqslant 1$, we thereby assume that a large part of the jet stream energy concentrates in this flow band. Next, keeping the expansion terms up to the first order of ϵ and λ, we arrive at the so-called thin-jet Lagrangian

$$\mathcal{L} = \int \left(\frac{\lambda}{\epsilon^2}(XY_t - YX_t) + \frac{\epsilon}{3}\gamma \frac{J_1}{J_0^2} \right) ds, \tag{44}$$

which describes large-scale dynamics of the jet meandering along the zero-buoyancy line.

To rewrite the thin-jet Lagrangian in a more elegant form, let us take a few more steps. First of all, for the self-consistency of perturbation theory in the first order, it is required that both terms on the left in the Lagrangian (44) have the same order. Whence, by comparing them, we get

$$\lambda = \epsilon^3/3. \tag{45}$$

Second, to obtain a closed description in the leading order of perturbation theory, we impose the conditions

$$X_s X_1 + Y_s Y_1 = 0, \quad X_s Y_2 - Y_s X_2 = 0, \tag{46}$$

which says that first-order displacements are orthogonal to the jet trajectory while second-order ones are parallel.

These constraints, if we take advantage of (42) and the complex notation

$$Z = X + iY, \tag{47}$$

allow us first to find that

$$X_1 + iY_1 = iJ_0/\overline{Z}_s \tag{48}$$

(the overline here and hereafter denotes complex conjugation), and then, based on (46), to get the expression

$$\frac{J_1}{J_0^2} = \text{Im}\left(\frac{1}{\overline{Z}_s} \partial_s \frac{1}{Z_s} \right). \tag{49}$$

After substituting (49) into (44), we can obtain the thin-jet Lagrangian in first order in ϵ. By taking out the common factor $\epsilon/3$ from it, we can present the final result in the closed form

$$\mathcal{L} = \text{Im} \int \left(\overline{Z}Z_t + \gamma \frac{1}{\overline{Z}_s} \partial_s \frac{1}{Z_s} \right) ds \tag{50}$$

in terms of the single complex variable Z. Note that the inertial terms $\hat{x}_t^2$ and $\hat{y}_t^2$ introduce corrections in this Lagrangian only in the fourth order in ϵ.

As known [22], the action principle with a Lagrangian of the type (50), sometimes called the phase-space action, leads directly to the equations in the canonical form

$$Z_t = 2i\frac{\delta\mathcal{H}}{\delta\overline{Z}}, \tag{51}$$

with the Hamiltonian

$$\mathcal{H} = \frac{1}{2} \, \mathrm{Im} \int \gamma \frac{1}{Z_s} \partial_s \frac{1}{\overline{Z}_s} ds. \tag{52}$$

Thus, the path equation that follows from (51) looks like

$$Z_t = \partial_s \left[\frac{1}{|Z_s|^4} \left(\gamma Z_{ss} - \frac{1}{2} \gamma_s Z_s \right) \right]. \tag{53}$$

Note also that, in terms of real dynamical variables X and Y, the Hamilton's formulation of (51) and (52) is equivalent to

$$X_t = -\frac{\delta \mathcal{H}}{\delta Y}, \quad Y_t = \frac{\delta \mathcal{H}}{\delta X}, \tag{54}$$

$$\mathcal{H} = \frac{1}{2} \int \gamma \frac{Y_{ss} X_s - X_{ss} Y_s}{\left(X_s^2 + Y_s^2 \right)^2} ds, \tag{55}$$

and instead of (53) yields the system of two equations

$$X_t = \partial_s \left(\frac{\gamma X_{ss} - \frac{1}{2} X_s \gamma_s}{\left(X_s^2 + Y_s^2 \right)^2} \right), \tag{56}$$

$$Y_t = \partial_s \left(\frac{\gamma Y_{ss} - \frac{1}{2} Y_s \gamma_s}{\left(X_s^2 + Y_s^2 \right)^2} \right). \tag{57}$$

IV. PARTICULAR SOLUTIONS

The simplest version of thin-jet dynamics is realized when the coefficient $\gamma(s)$ characterizing the temperature gradient across the jet becomes a constant. In this case, the transformation $s \to s\gamma$ allows us to exclude it and simplify Eq. (53) to the form

$$Z_t = \partial_s (Z_{ss} |Z_s|^{-4}). \tag{58}$$

If the contributions from integrating at endpoints are absent or mutually compensated, as in the case of a closed contour, then in addition to the Hamiltonian $\mathcal{H}$, conserved automatically, the thin-jet model provides a time invariance of two more integrals:

$$I_1 = \int |Z|^2 ds, \quad I_2 = \mathrm{Im} \int \overline{Z}_s Z ds. \tag{59}$$

Since the integral I_2 implies a surface area surrounded by the zero-buoyancy contour, its conservation needs an explanation because, generally speaking, due to the two-dimensional compressibility in the full model (1)–(4), this quantity is not conserved. It is invariant only in the first order of perturbation theory, because in this approximation $h = H + O(\epsilon)$ and the fluid can be considered practically incompressible.

Equation (58) possesses a number of symmetries leaving it unchanged under obvious transformations:

$$t \to t + t_0, \quad s \to s + s_0, \tag{60}$$

$$Z \to Z + Z_0, \quad Z \to e^{i\varphi} Z, \tag{61}$$

$$Z(-s, -t) \to Z(s, t), \tag{62}$$

which mean invariance under space-time translations, rotations, and inversions. Here t_0, s_0, Z_0 are arbitrary constants.
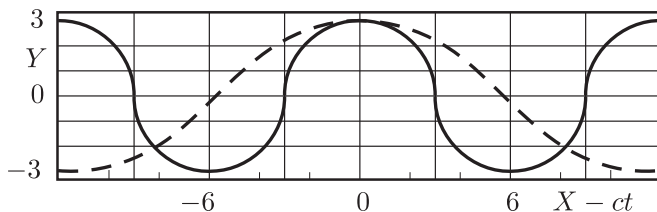
FIG. 1. Periodic steady-state solutions. Both solutions oscillate with the same amplitude $a = 3$. The solid line corresponds to $m = 1$, while the dotted line corresponds to $m = 0.5$.

In addition, Eq. (58) is scale invariant with respect to the transformation

$$(s, t, Z) \rightarrow (\alpha s, \tau t, (\alpha \tau)^{1/4} Z), \tag{63}$$

where the constants α and τ are rescaling factors. This symmetry is responsible for the conservation of the integral

$$I_3 = \text{Im} \int \overline{Z}(3tZ_t + sZ_s)ds, \tag{64}$$

Consider some solutions of Eq. (58). Let $X = s$, i.e., s coincides with the axis X, then this equation yields

$$Y_t = \partial_s \frac{Y_{ss}}{\left(1 + Y_s^2\right)^2}. \tag{65}$$

Let us look for steady-state solutions $Y(\sigma)$, $(\sigma = s - ct)$ propagating with a constant velocity c without profile deformation along the X axis. In this case, Eq. (65) can be integrated twice and, by using the shift $Y \rightarrow Y + Y_0$, is transformed to the form

$$cY^2 - \frac{1}{1 + Y_\sigma^2} + c_1 = 0, \tag{66}$$

where the integration constant c_1 must be chosen depending on how the solution behaves at infinity.

A. Oscillating jets

In the case of periodic behavior with an amplitude a, by assuming $Y(0) = a$ and $Y_\sigma(0) = 0$, one can find that $c_1 = 1 - ca^2$, so solutions can be sought as steady-state waves

$$Y = a \cos \theta, \quad \theta = \theta(\sigma). \tag{67}$$

After substituting Eq. (67) into Eq. (65) and integrating, we get

$$\theta_\sigma^2 = \frac{c}{1 - ca^2 \sin^2 \theta}. \tag{68}$$

As the analysis shows, periodic steady-state solutions exist under the condition $0 < c < 1/a^2$. Being represented in a parametric form

$$Y = a \cos \theta, \quad X = ct + \frac{a}{\sqrt{m}} E(\theta | m), \tag{69}$$

they describe the nonlinear waves shown in Fig. 1. Here E is an incomplete elliptic integral of the second kind with parameter $0 < m < 1$, which is related to a and c as
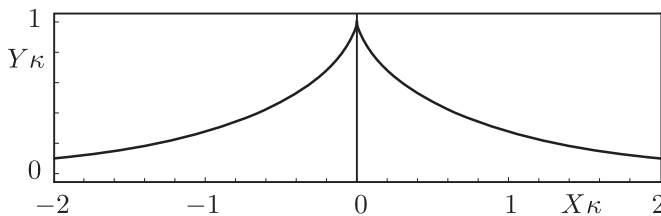
$$m = ca^2. \tag{70}$$

FIG. 2. The cusped steady-state solution.

Note that, when $a \to 0$, the solution (69) becomes

$$Y = a\cos(\sqrt{c}\sigma), \quad X = ct + \sigma \tag{71}$$

and describes a weakly oscillating jet. When $a = 0$, we get the trivial result $Y = 0$, $X = ct + \sigma$, which describes a straight-line jet and coincides with what follows in the first approximation from the expansion (30) in powers of ϵ. The stability of oscillating solutions in the long-wave approximation ($m \to 0$) is discussed in the Appendix.

B. Cusped jets

For the case of nonperiodic behavior, when solutions decrease at infinity as $Y \sim e^{-\kappa|\sigma|}$, where κ is some positive constant, we find that

$$c_1 = 1, \quad c = -\kappa^2. \tag{72}$$

In this case, Eq. (65) admits the nonsmooth so-called cusped solutions (cuspons). The corresponding trajectories of jets can be described parametrically by the expression

$$\sigma = X + \kappa^2 t = \mp \frac{1}{\kappa}(\sqrt{1 - \kappa^2 Y^2} - \text{arcth}\sqrt{1 - \kappa^2 Y^2}), \tag{73}$$

where Y changes in the range $0 < Y < 1/\kappa$. As shown in Fig. 2, although such solutions take a finite value $Y(0) = 1/\kappa$ at the peak point $\sigma = 0$, all their derivatives become singular there. In particular, the first derivative in the vicinity of this point looks like

$$Y_\sigma \approx -(3\kappa|\sigma|)^{-1/3}\,\text{sign}\,\sigma. \tag{74}$$

Note that cusped solutions are Lyapunov stable due to the negativity of their propagation velocity c (see Appendix).

C. Spiral jets

By relaxing some of the restrictions, it is possible to significantly extend the class of solutions. In particular, the solutions describing spiral jets turn out to be among them. To construct something similar, let us use the ansatz

$$Z = c\sigma^p(t_0 - t)^m, \quad \sigma = \gamma s, \quad 0 \leqslant t \leqslant t_0, \tag{75}$$

assuming that c and t_0 are real while p and m are complex parameters. Here we have to note that, under the above conditions, the solution (75) exists only when $\sigma = \gamma s > 0$ and has a finite lifetime t_0, so that at $t = t_0$ it disappears, collapsing into a point.

Substituting (75) into Eq. (58) yields the set of constraints

$$\overline{m} + m = \tfrac{1}{2}, \quad \overline{p} + p = \tfrac{1}{2}, \quad 2\overline{p} + p - 2 = c^4 pm\overline{p}^2. \tag{76}$$
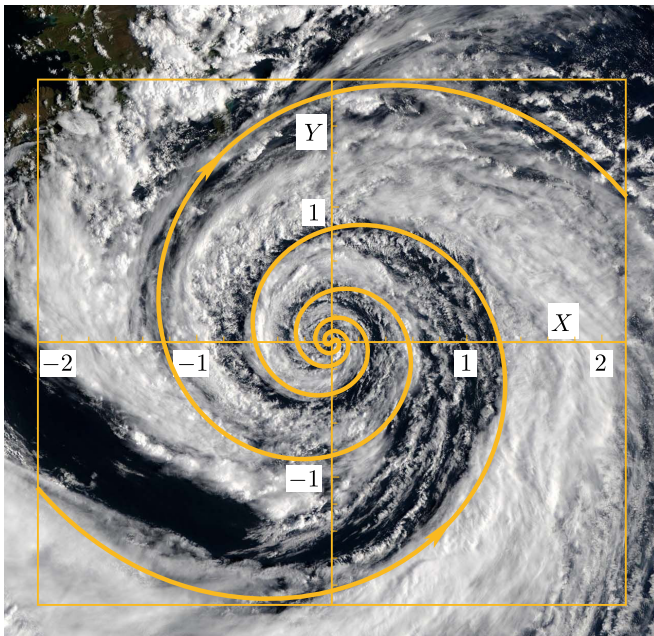
FIG. 3. Two-armed spiral solution for $\nu = -4$ and $\varphi_0 = \pi$. A satellite image of an occluded front wrapping-up in a spiral is used as the background for comparison.

Solving these equations, we obtain

$$p = \frac{1}{4}(1 + i\nu), \quad m = \frac{1}{4}\left(1 + i\frac{\nu}{3}\frac{13 + \nu^2}{5 + \nu^2}\right), \tag{77}$$

$$c = 2 \times 3^{1/4}(5 + \nu^2)^{1/4}(1 + \nu^2)^{-1/2}, \tag{78}$$

where ν is a free real parameter.

By separating the variables and writing the space part of the solution (75) as

$$\sigma^{(1+i\nu)/4} = \varrho e^{i\varphi}, \tag{79}$$

it is easy to find that

$$\varphi = \frac{\nu}{4}\ln\sigma, \quad \varrho = e^{\varphi/\nu}, \tag{80}$$

so the solutions (75) describe logarithmic spirals (see Fig. 3).

Obviously, within one-armed spiral solutions, the existence condition $\sigma > 0$ can be fulfilled either if $\gamma > 0$ and $s > 0$, or if $\gamma < 0$ and $s < 0$. However, in any case, one-armed solutions turn out to be formal. Indeed, supposing $0 < \sigma < A$ and calculating the Hamiltonian H, we find

$$\mathcal{H} = \frac{2A^{3/2}\nu}{3\sqrt{3}\gamma\sqrt{1 + \nu^2}}(t_0 - t)^{-1/2}. \tag{81}$$

Thus, the Hamiltonian H for one-armed spiral solutions is time dependent and divergent when $A \to \infty$ or $t \to t_0$.

To remedy this defect, we consider two-armed spiral solutions. In these solutions, on the one arm, the parameter γ is positive and s runs from zero to infinity, while on the other arm, γ is negative and s runs from zero to minus infinity. As follows from (81), the total contribution to the Hamiltonian for such solutions is zero.

In addition, to avoid overlapping spiral arms in (X, Y)-coordinate space, it is necessary to multiply one of the solutions by $e^{i\varphi_0}$. Without any impact on anything else, this operation merely rotates one of the spiral arms by some constant angle φ_0. Recall that such a possibility always exists due to the rotational invariance of the solutions.

The two-armed solution thus obtained is shown in Fig. 3 against the background of an occluded spiral front in the atmosphere. As the parameter γ takes different signs on different spiral arms, the velocities on them, marked by arrows, also have opposite directions.

Another property possessed by the spiral solution is rotation. The basis for this conclusion becomes evident if to extract from the solution only that its part responsible for the temporal evolution:

$$Z \sim (t_0 - t)^{1/4} e^{i\mu \ln (t_0 - t)}, \quad \mu = \frac{\nu}{12} \frac{13 + \nu^2}{5 + \nu^2}, \tag{82}$$

The right-hand side of (82) indicates that, along with collapse, the two-armed spiral also performs a nonuniform rotation with angular velocity

$$\Omega = \mu(t - t_0)^{-1}. \tag{83}$$

V. CONCLUSIONS

In this paper, an approximate nonlinear model has been derived to describe the dynamics of thin jets arising at temperature fronts and moving along zero-buoyancy lines. Although the model is obtained under few simplifications, it has some predictive power and possesses a potential for further development. The results reached within this model turn out to be useful in many aspects.

First, they show that motion equations describing the dynamics of thin jets along temperature fronts and ones along potential vorticity fronts are fundamentally different from each other. What is remarkable, however, is that despite this, both theories predict the same $L \sim T^{1/3}$ relationship between the characteristic scales of length L and time T.

Second, the obtained solutions may serve as a kind of benchmark for subsequent analytical and numerical studies. In particular, in this capacity, they can be in demand when creating more advanced models of thin jets, which will take into account the layer thickness changes and the beta effect. The stability problem was concerned only in the narrow context of the stationary solutions considered in this work (see Appendix).

Another intriguing but yet unsolved question is the existence of collapsing solutions for closed-loop jets. If it were an isotropic collapse, the problem could be resolved trivially because the equation (58) formally admits the self-similar substitution

$$Z = (t_0 - t)^k Z(\sigma), \quad \sigma = s(t_0 - t)^{1-4k}, \tag{84}$$

where k is a parameter and t_0 is the collapse time, during which the jet contour contracts into a point. But because the surface-area conservation law $I_2 = $ const. forbids such behavior, the anisotropic collapse scenario seems more plausible [13]. As a result of such a scenario, the region within a closed jet should shrink not into a point but an infinitely extended line.

The data that support the findings of this study are available within the article.

ACKNOWLEDGMENTS

APPENDIX: STABILITY OF STATIONARY SOLUTIONS

First of all, note that the path equation in one variable version (65) can be presented as

$$Y_t = \partial_s \frac{Y_{ss}}{\left(1 + Y_s^2\right)^2} = \partial_s \frac{\delta \mathcal{G}}{\delta Y}, \tag{A1}$$

where

$$\mathcal{G} = -\frac{1}{2} \int Y_s \arctan (Y_s) ds, \tag{A2}$$

and hence it also belongs to a Hamiltonian type.

Stationary solutions $Y = Y(\sigma), \sigma = s - ct$ can be viewed as an equilibrium point in the infinite-dimensional phase space of the variable Y. Indeed, in this case, the equation of motion which follows from (A1) and (A2) can be reduced to the variational problem

$$\delta(\mathcal{G} + cP) = 0, \quad P = \frac{1}{2} \int Y^2 ds, \tag{A3}$$

which indicates that, for these solutions, the extremum of the functional $\mathcal{G}$ is reached at the fixed integral P.

By the Lyapunov stability theorem (see, e.g., Refs. [23,24]), a stationary point of a Hamiltonian system is stable if it is a maximum or minimum point of the Lyapunov functional

$$\Lambda = \mathcal{G} + cP. \tag{A4}$$

If the stationary point is a saddle, then the equilibrium state is unstable.

Because, in our case, the quantity $\mathcal{G}$ is a negative definite, note that, for solutions with negative velocities, the Λ functional will also be negative definite. Consequently, the cusped solutions with $c < 0$ from Sec. IV are Lyapunov stable. The stability of the wave solutions with $c > 0$ turns out to be a more complicated problem.

There is a specific technique for studying the stationary point type (see Ref. [25] and references therein). This technique relies on using transforms, which contain a continuous dependence on parameters and leave the integral of motion P invariant. After employing such transforms, the Hamiltonian $\mathcal{G}$ becomes a usual function of parameters, making it easy to determine the type of a stationary point.

To apply this method to nonlinear $2L$-periodic stationary solutions in the long-wave approximation $Y_s^2 \ll 1$, let us replace the Hamiltonian $\mathcal{G}$ by its expansion. Then, limiting ourselves to the first two terms, we obtain

$$\mathcal{G} = -\frac{1}{2} I_1 + \frac{1}{6} I_2, \quad P = \frac{1}{2} \int_{-L}^{L} Y^2 ds, \tag{A5}$$

$$I_1 = \int_{-L}^{L} Y_s^2 ds, \quad I_2 = \int_{-L}^{L} Y_s^4 ds. \tag{A6}$$

As one possible transforms leaving P invariant, we will consider the scaling transform

$$Y \rightarrow \alpha^{-1/2} Y(s/\alpha), \quad L \rightarrow \alpha L, \tag{A7}$$

where $\alpha > 0$ is a parameter. In this way, the Hamiltonian $\mathcal{G}$ becomes a function of the parameter α,

$$\mathcal{G} = -\frac{I_1}{2\alpha^2} + \frac{I_2}{6\alpha^5}. \tag{A8}$$

By analogy with Ref. [25], we can find that the integrals I_1 and I_2 and the momentum P are tied together by the relations

$$2cP - I_1 + \tfrac{2}{3} I_2 = 0, \quad -2cP - I_1 + I_2 = 0. \tag{A9}$$

Here the first follows from the variational principle (A3) and the second from the virial theorem [25]. As a result, we have $I_1 = 10cP$, $I_2 = 12cP$, and thus, comes to the expression

$$\mathcal{G} = cP\left(-\frac{5}{\alpha^2} + \frac{2}{\alpha^5}\right), \qquad (A10)$$

which has a minimum $\mathcal{G}_{\min} = -3cP$ at $\alpha = 1$. This fact points to the stability of periodic solutions with respect to perturbations retaining scale symmetry, at least, in the long-wave approximation.

[1] A. R. Robinson and P. P. Niiler, The theory of free inertial jets: I. Path and structure, Tellus **19**, 269 (1967).

[2] J. R. Luyten and G. Flierl, On the theory of thin rotating jets: A quasi-geostrophic time-dependent mode, Geophys. Fluid Dyn. **6**, 211 (1975).

[3] G. R. Flierl and A. R. Robinson, On the time dependent meandering of a thin jet, J. Phys. Oceanogr. **14**, 412 (1984).

[4] L. J. Pratt and M. E. Stern, Dynamics of potential vorticity fronts and eddy detachment, J. Phys. Oceanogr. **16**, 1101 (1986).

[5] L. J. Pratt, Meandering and eddy detachment according to a simple (looking) path equation, J. Phys. Oceanogr. **18**, 1627 (1988).

[6] B. Cushman-Roisin, L. J. Pratt, and E. A. Ralph, A general theory for equivalent barotropic thin jets, J. Phys. Oceanogr. **23**, 91 (1993).

[7] J. Nycander, D. G. Dritschell, and G. G. Sutyrin, The dynamics of long frontal waves in the shallow water equations, Phys. Fluids A **5**, 1089 (1993).

[8] E. A. Ralph and L. J. Pratt, Predicting eddy detachment for an equivalent barotropic thin jet, J. Nonlinear Sci. **4**, 355 (1994).

[9] B. Cushman-Roisin, J. A. Proehl and D. T. Morgan, Barotropic thin jets over arbitrary topography, Dyn. Atmospheres Oceans **26**, 73 (1997).

[10] P. Ripa, Conservation laws for primitive equations models with inhomogeneous layers, Geophys. Astrophys. Fluid Dyn. **70**, 85 (1993).

[11] P. Ripa, On improving a one-layer ocean model with thermodynamics, J. Fluid Mech. **303**, 169 (1995).

[12] E. S. Warneford and P. J. Dellar, The quasi-geostrophic theory of the thermal shallow water equations, J. Fluid Mech. **723**, 374 (2013).

[13] V. P. Goncharov and V. I. Pavlov, Simple model of the Rayleigh-Taylor instability, collapse, and structural elements, Phys. Rev. E **88**, 023002 (2013).

[14] D. L. T. Anderson, An advective mixed-layer model with applications to the diurnal cycle of the low-level East-African jet, Tellus, Ser. A **36**, 278 (1984).

[15] P. Ripa, On the validity of layered models of ocean dynamics and thermodynamics with reduced vertical resolution, Dyn. Atmospheres Oceans **29**, 1 (1999).

[16] R. Salmon, Practical use of Hamilton's principle, J. Fluid Mech. **132**, 431 (1983).

[17] R. Salmon, Hamiltonian fluid mechanics, Annu. Rev. Fluid Mech. **20**, 225 (1988).

[18] D. W. McLaughlin and A. C. Scott, A multisoliton perturbation theory, in *Solitons in Action*, edited by K. Lonngren and A. Scott (Academic Press, New York, 1978), pp. 201–256.

[19] L. P. Gor'kov and N. B. Kopnin, Viscous vortex flow in superconductors with paramagnetic impurities, Zh. Eksp. Teor. Fiz. **60**, 2331 (1971) [Sov. Phys. JETP **33**, 1251 (1971)].

[20] R. Rajaraman, *Solitons and Instantons: An Introduction to Solitons and Instantons in Quantum Field Theory* (North-Holland Publishing Company, Amsterdam, 1982).

[21] V. P. Goncharov and V. M. Gryanik, Dynamics of solitary dissipative vortices: Vortex lattices and their stability, Zh. Eksp. Teor. Fiz. **91**, 1653 (1986) [Sov. Phys. JETP **64**, 976 (1986)].

[22] P. J. Morrison, Hamiltonian description of the ideal fluid, Rev. Mod. Phys. **70**, 467 (1998).

[23] D. D. Holm, J. E. Marsden, T. Ratiu, and A. Weinstein, Nonlinear stability of fluid and plasma equilibria, Phys. Rep. **123**, 1 (1985).

[24] H. D. I. Abarbanel, D. D. Holm, J. E. Marsden, and T. S. Ratiu, Nonlinear stability analysis of stratified fluid equilibria, Philos. Trans. R. Soc. London A **318**, 349 (1986).

[25] E. A. Kuznetsov, A. M. Rubenchik, and V. E. Zakharov, Soliton stability in plasmas and hydrodynamics, Phys. Rep. **142**, 103 (1986).